DFIG-BASED WIND TURBINE GENERATOR PERFORMANCE ANALYSIS FOR WIND SPEED VARIATION

Article · March 2021

CITATIONS
0

READS
248

4 authors:

Dahiru Musbahu
Federal University of Technology Minna
3 PUBLICATIONS **1** CITATION
SEE PROFILE

Gbenga Olarinoye
Ahmadu Bello University
31 PUBLICATIONS **66** CITATIONS
SEE PROFILE

Adamu Saidu Abubakar
Ahmadu Bello University
47 PUBLICATIONS **182** CITATIONS
SEE PROFILE

Abubakar Umar
Ahmadu Bello University
49 PUBLICATIONS **58** CITATIONS
SEE PROFILE

DFIG-BASED WIND TURBINE GENERATOR PERFORMANCE ANALYSIS FOR WIND SPEED VARIATION

D. Musbahu[1], G.A Olarinoye[2], A.S Abubakar[3], U Abubakar[4], B.B Idrees[5]

[1]School of Electrical and Electronic Engineering, FUT Minna-Nigeria.
[2, 3]Electrical Engineering Department, Ahmadu Bello University, Zaria-Nigeria
[4]Computer Engineering Department, Ahmadu Bello University, Zaria-Nigeria.
[5]Electrical Engineering Department, Nile University of Nigeria, Abuja-Nigeria.
dahirumisbahu@gmail.com

Keywords: –
DFIG-Modeling, Wind Turbine Model, Rotor Side Converter (RSC), ISC (Indirect Speed Control), Grid Side Converter (GSC)

Received: January, 2021.
Reviewed: February, 2021
Accepted: February, 2021
Published: March, 2021

ABSTRACT

Wind unit in power system over the last decades has received global attention as compared to other renewable sources because of its emission free nature. This paper performs an evaluation of Doubly-Fed Induction Generators (DFIG)-based wind turbine under different wind speeds variation in synchronous rotating reference frame. Many authors have presented similar models but this paper develops a Simulink model for the DFIG by using the analytical equations of the DFIG instead of the single DFIG block contained in the Simscape library of the Simulink software. The control strategy was also implemented using appropriate function blocks in the Simulink environment and some MATLAB scripts. Maximum Power Point Tracking (MPPT) technique was applied to wind turbine and it extracts optimal power from the wind. Proportional Integral (PI) controller has been used to stabilize the system against wind speed fluctuations. The rotor speed response after connecting it to the wind speed changed from 8 m/s to 10 m/s was provided. The voltage of the DC link was controlled to a constant value of 1150 V for a constant rotor power, while the reactive power of the rotor was regulated at 0 VAR thereby ensuring that no reactive power was exchanged with the grid. Simulation results has shown that the effectiveness of DFIG-based wind turbine to operate at different wind speed conditions to capture more power from the wind.

1. INTRODUCTION

The increasing demand for electric energy around the world has a high motivation in the use of wind, a variant of renewable energy source. The known energy sources are scarce, and this results to pollution of the environment. Recently, research has focused on maximum use of renewable energy sources like wind, solar energy and fuel cell. Wind energy is a fast research area and clean energy source with respect to others, due to its emission free nature [1, 2]. From Global Wind Energy Council (GWEC) statistics, the installed capacity of wind power plants worldwide has go beyond 318GW since 2013 and it was estimated to be about 712GW since last year [3]. The wind turbines has importance in obtaining wind energy from the moving air, which is a significant achievement in modern power system with minimum negative effect on environment which makes it become people alternative energy source [4].

Nowadays DFIG are frequently used for large wind power generation due to its ability of variable speed operation in which 20%-30% power rating pass through power electronic converter. This causes a significant reduction in the converter size, thereby resulting to significant system cost benefit. This makes it necessary to optimize the extracted power from the wind as the DFIG rotor speed changes proportionally to that of the wind speed [5].

Over the past decade, DFIG has proven to be mostly preferred generating system with wind turbine as it provides the control of active and reactive exchanged with the network and they have high efficiency, low cost and flexible control.

A lot research has been carried out based on wind energy conversion system (WECS), which is one of the recent research area in renewable energy source. Yang, Wu [6] developed a hybridized mechanical-electrical DFIG Wind Turbine Model. A typical 1.5MW DFIG-based wind turbine was modeled using MATLB/Simulink and FAST. In the work of Chatterjee and Rather [7], DFIG-based Variable Speed Wind Turbine was modeled and controlled in which steady state operation of the DFIG was investigated. Lavanya, Sekhar [8] proposed a study of the performance of Indirect Matrix Converter with improved control supplying to the rotor of Doubly Fed Induction Machine (DFIM) as motor or generator operational mode. Fig 1 shows a WECS system equipped with the DFIG.

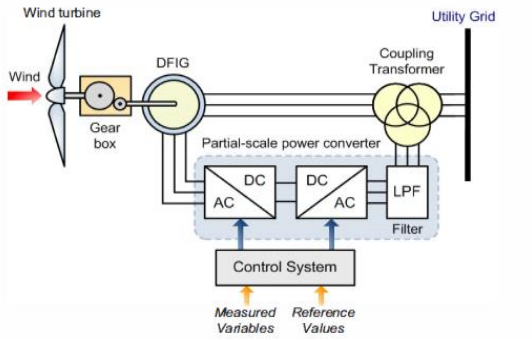

Fig. 1: DFIG wind turbine system

The variable speed operation was derived by the injection of a variable voltage into the rotor at slip frequency. Also, the injected rotor voltage was derived by the use of two AC/DC insulated gate bipolar transistor (IGBT) based Voltage Source Converter (VSC) through a PWM (power converter and inverter equipped with the passive filter placed on the chain) with dc-link in between. Vector control strategy provide the control of DFIG and the filter which is PI based controllers [9].

This paper is aimed at evaluating the performance of DFIG based wind turbine with view of extracting a maximum power under various wind speed operation in MATLAB/SIMULINK 2018a environment.

2. MATERIALS AND METHODS

The DIFIG-based wind turbine configuration include the electrical parts (which includes the DFIG and the back-back converter set) and the mechanical parts (which includes the aerodynamic system with rotor blades and the gear box).

2.1 The Turbine Model

The power (mechanical) captures or derived by turbine blades are given as [10]:

$$P_m = \frac{1}{2}\rho\pi R^2 C_p(\lambda,\beta)V_w{}^3 \quad (1)$$

Where: ρ is air density in (kg/m^3), the Radius of wind turbine blade (m) is R, the wind speed in (m/sec) is V_w, while C_p and β are the power coefficient and pitch angle of the wind turbine respectively.

Also λ is the tip speed ratio which is defined as the ratio of the angular rotor speed of the wind turbine to the linear wind speed at the tip of the blades, and is given as:

$$\lambda = \frac{w_r R}{V_w} \quad (2)$$

w_r is the rotor speed in (rad/sec). The equation of the driving torque expression is given by equation (3) as [11]:

$$T_m = \frac{1}{2}\rho ARC_T V_w{}^2 \quad (3)$$

Where C_T is the torque coefficient expressed as follows [11]:

$$C_T = \frac{C_p}{\lambda} \quad (4)$$

The coefficient C_p is calculated based on variable speed wind turbine (VSWT) as follows [11]:

$$\lambda_i = \frac{1}{\frac{1}{\lambda + 0.002\beta} - \frac{0.03}{\beta^3 + 1}} \quad (5)$$

$$C_p(\lambda,\beta) = 0.73\left[\frac{151}{\lambda} - 0.58\lambda - 0.002\beta^{2.14} - 13.2\right]e^{\frac{184}{\lambda_i}} \quad (6)$$

An Indirect speed control (ISC) was adopted for extracting the maximum power from the wind by designing MPPT controller based on Fig. 2.

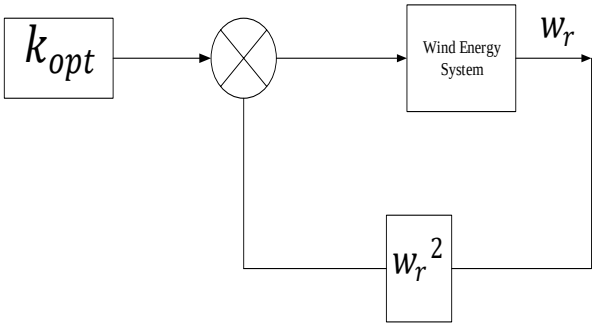

Fig. 2: MPPT controller

The reference electromagnetic torque from the output of the controller is expressed as follows:

$$T = \frac{1}{2}\rho\pi R^5 \frac{(C_p)\max}{(\lambda_{opt})^3} w_r^2 \quad (7)$$

Where, λ_{opt} represents the tip speed ratio which is usually tuned to optimal value over a wide range of wind speed. The electromagnetic reference is also given as:

$$T = k_{opt} w_r^2 \quad (8)$$

Where $w_r = \Omega_t$ is rotor rotational speed obtained from the generator shaft, which is given as:

$$k_{opt} = \frac{1}{2}\rho\pi R^5 \frac{(C_p)\max}{(\lambda_{opt})^3} w_r^2 \quad (9)$$

Therefore equation (9) lead to the controller design that was illustrated in Fig. 2.The turbine aerodynamic was presented in Fig. 3.

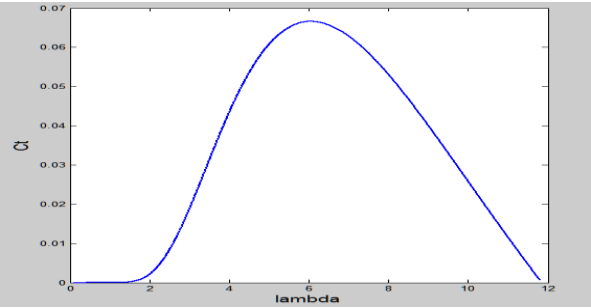

(a) Torque coefficient- tip-speed ratio

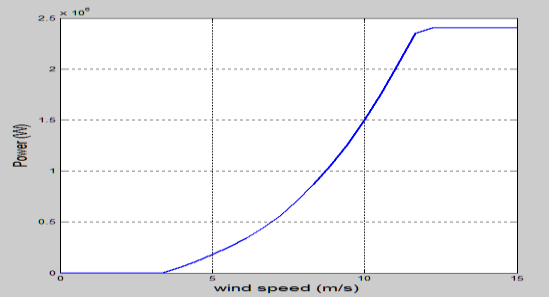

(b) Turbine output power-wind speed

Fig. 3: The Wind Turbine Aerodynamic

The Torque coefficient (C_t) with respect to tip-speed (λ) ratio was shown in Fig. 3(a). The wind turbine operates optimally and tracks power (maximum) from the wind keeping tip speed ratio (λ_{opt}) at its optimal value of 7.2. Also the mechanical power associated with the wind turbine was proportional to the wind speed as illustrated in Fig. 3.1(b).

2.2 DFIG Modeling

The topology of DFIG was illustrated in Fig. 1. There is a direct connection of the stator to the

grid, while the rotor was indirectly connected to the grid by a back-to-back voltage source converter (VSC). Converter configuration includes rotor inverter (RSI) and grid converter (GSC) with capacitor in between. The $d-q$ equivalent circuit diagram of the DFIG machines is shown in Fig. 4 [12, 13].

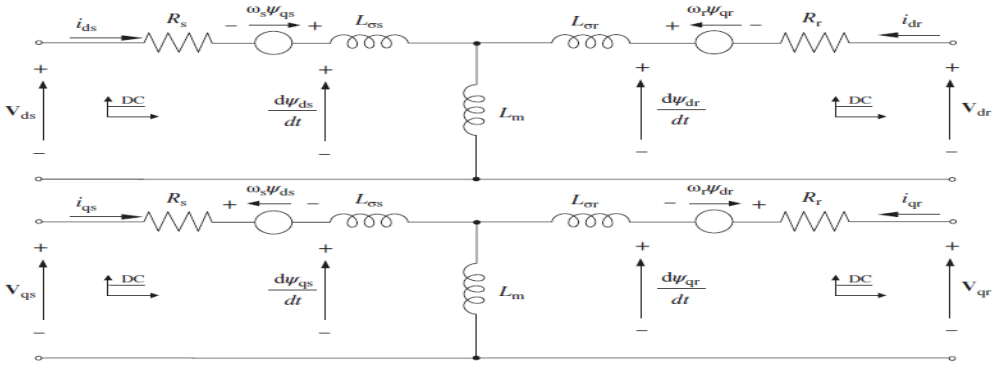

Fig. 4: The d-q equivalent circuit of a DFIG

Based on the equivalent DFIG circuit of Fig. 4, model equations of voltages and flues in $d-q$ reference frame given as:

$$\begin{cases} V_{ds} = R_s i_{ds} + \dfrac{d\psi_{ds}}{dt} - jw_s\psi_{qs} \\ V_{qs} = R_s i_{qs} + \dfrac{d\psi_{qs}}{dt} + jw_s\psi_{ds} \end{cases} \quad (10)$$

$$\begin{cases} V_{dr} = R_r i_{dr} + \dfrac{d\psi_{dr}}{dt} - jw_r\psi_{qr} \\ V_{qr} = R_r i_{qs} + \dfrac{d\psi_{qr}}{dt} + jw_r\psi_{dr} \end{cases} \quad (11)$$

$$\begin{cases} \psi_{ds} = L_s i_{ds} + L_m i_{dr} \\ \psi_{qs} = L_s i_{qs} + L_m i_{qr} \end{cases} \quad (12)$$

$$\begin{cases} \psi_{dr} = L_r i_{dr} + L_m i_{ds} \\ \psi_{qs} = L_r i_{qr} + L_m i_{qr} \end{cases} \quad (13)$$

Where, quantities R_s and R_r represents the stator and rotor resistance, L_m is the mutual inductance, w_s is the synchronous (stator) frequency, L_s and L_r denotes the stator and rotor inductance respectively. s and r Subscript represents the stator and rotor variables. However, V_s, i_s and ψ_s are the stator voltage, current and stator flux respectively. Also, V_r, i_r and ψ_r denotes the rotor voltages, current and flux vectors respectively.

The power expressions of the DFIG are given as:

$$P_s = 1.5\left(V_{ds} i_{ds} + V_{ds} i_{ds}\right) \quad (14)$$

$$P_r = 1.5\left(V_{dr} i_{dr} + V_{dr} i_{dr}\right) \quad (15)$$

$$Q_s = 1.5\left(V_{qs} i_{ds} - V_{ds} i_{qs}\right) \quad (16)$$

$$Q_r = 1.5\left(V_{qr} i_{dr} - V_{dr} i_{qr}\right) \quad (17)$$

Where P and Q donate active and reactive component of power in stator with 's' and rotor with 'r' subscripts.

2.3 DFIG Control Technique

Vector control technique are applied DFIG AC-DC-AC converter so as to ensure the active control of grid active and reactive power of the DFIG [14]. The converter is a bidirectional converter made up of a rotor side rectifier and the grid side inverter with DC-link in between and both with conventional pulse width modulation (PWM) [6].

2.3.1 Rotor Side Converter Model

The rotor side converter model with the help of vector control ensures control of stator power (active and reactive) using PI controller through control of rotor direct and quadrature current components under stator flux orientation [15, 16]. Fig. 5 illustrates the block diagram of RSC control

.

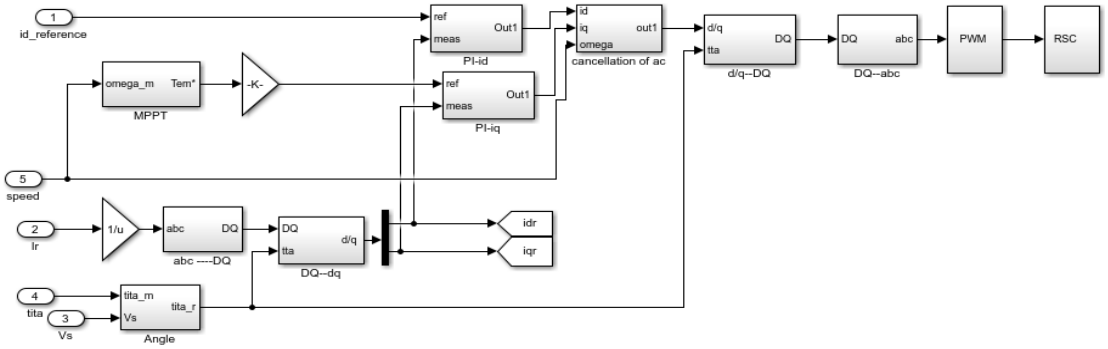

Fig. 5: Block Diagram of the Rotor Side Converter Control

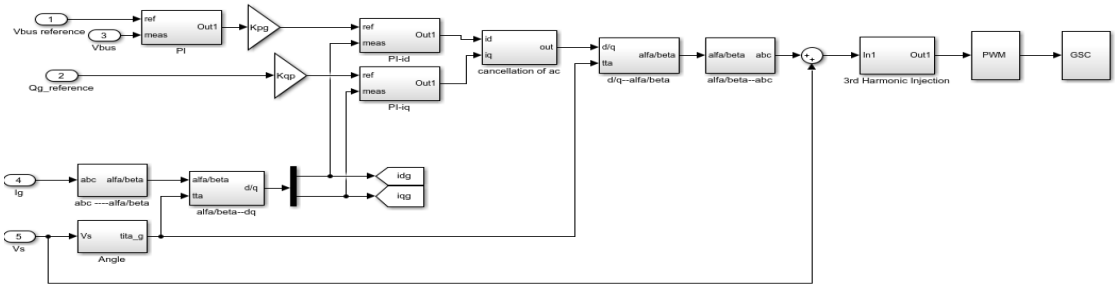

Fig. 6: Block Diagram of the Grid Side Converter.

2.3.2 Grid Side Converter Model

Similarly, a grid side converter GSC ensures the control of DC bus voltage, reactive power exchange between the grid side converter and the grid. The space vector voltage V_g of the grid is in accordance with the $d-axis$ of the dq rotating reference frame and the relevant equation of the control scheme are discussed in [17]. Fig. 6 shows the control block of the grid side inverter.

2.3.3 PI Controller Model

The RSC and GSC each consists of two control loops (inner and outer control loops). The RSC inner control loop regulates the $d-q$ rotor current component using PI controller for each current component [17]. The detail PI controller design for outer control of RSC and GSC control are discussed in [18].

The inner control loop controllers were designed using $d-q$ rotor voltage equation as follows:

$$V_{dr} = R_r i_{dr} + \sigma L_r \frac{d}{dt} i_{dr} - w_r \sigma L_r i_{qr} + \frac{L_m}{L_s} \frac{d}{dt} \left| \vec{\psi}_s \right| = V_{dr}^{\ 1} + V_{dr}^{\ 2} \quad (18)$$

$$V_{qr} = R_r i_{qr} + \sigma L_r \frac{d}{dt} i_{qr} - w_r \sigma L_r i_{dr} + \frac{L_m}{L_s} \frac{d}{dt} \left| \vec{\psi}_s \right| = V_{qr}^{\ 1} + V_{qr}^{\ 2} \quad (19)$$

Where; $V_{dr}{}^{1}$ and $V_{qr}{}^{1}$ are called current regulation parts and are given as:

$$V_{dr}{}^{1} = R_r i_{dr} + \sigma L_r \frac{d}{dt} i_{dr} \quad (20)$$

$$V_{qr}{}^{1} = R_r i_{qr} + \sigma L_r \frac{d}{dt} i_{qr} \quad (21)$$

:

For each rotor current component $(d-q)$, a PI controller was designed as shown in Fig. 7. The transfer function of the rotor current components in Laplace transform is

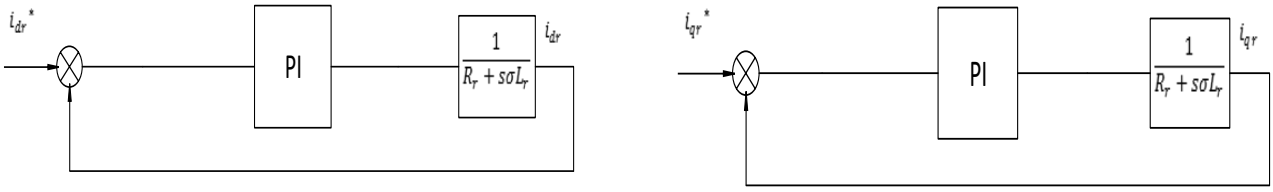

$d-$Current Control

$q-$ Current Control

Fig. 7: The Block Diagrams of Rotor Currents control

$$\frac{i_{dr}}{i_{dr}*} = \frac{sK_p + K_i}{s^2(\sigma L_r) + s(R_r + K_p) + K_i} \quad (22)$$

$$\frac{i_{qr}}{i_{qr}*} = \frac{sK_p + K_i}{s^2(\sigma L_r) + s(R_r + K_p) + K_i} \quad (23)$$

The rotor current control loop dynamic can be approximated by a second-order system dynamics

The denominator of equation (22) and (23) can be matched with the denominator of second-order system as follows:

$$s^2(\sigma L_r) + s(R_r + K_p) + K_i = s^2 + 2\xi w_n s + w_n{}^2 \quad (24)$$

Where w_n is the natural frequency in rad/s, and ζ the damping ratio. By normalizing (24) and equating coefficient the PI controller gains K_p and K_i were evaluated as follows:

$$s^2 + \left(\frac{R_r + K_p}{\sigma L_r}\right)s + \frac{K_i}{\sigma L_r} = s^2 + 2\xi w_n s + w_n{}^2 \quad (25)$$

Equating coefficient:

$$\frac{R_r + K_p}{\sigma L_r} = 2\xi w_n \quad (26)$$

$$\frac{K_i}{\sigma L_r} = w_n{}^2 \quad (27)$$

Therefore,

$$\begin{cases} K_p = 2\xi w_n \sigma L_r - R_r \\ K_i = \sigma L_r w_n{}^2 \end{cases} \quad (28)$$

Where, L_r, R_r are the rotor inductance, rotor resistance, and K_p, K_i are PI controller gains. The system was chosen to be critically damped and close loop poles of the system (w_n) to be faster than open-loop poles were $w_n = \frac{\sigma L_r}{R_r}$ as follows:

$$\xi = 1 \quad (29)$$

$$w_n = \frac{x}{\frac{\sigma L_r}{R_r}} \tag{30}$$

3. RESULTS AND DISCUSSION.

MATLAB/Simulink 2018a environment was used to model and simulate the configuration 2MW DFIG-based wind turbine WECS. The simulation was carried out on two different wind speed and the performance evaluations of various parameter of the machine were analyzed as follows:

The mechanical rotor speed and the electromagnetic torque responses were depicted in Fig. 8 and Fig. 9 respectively for 8m/s of wind the speed. The system attained steady state operation point at t = 6 second. Fig. 10 depicts the corresponding stator and rotor voltage, current, active and power responses.

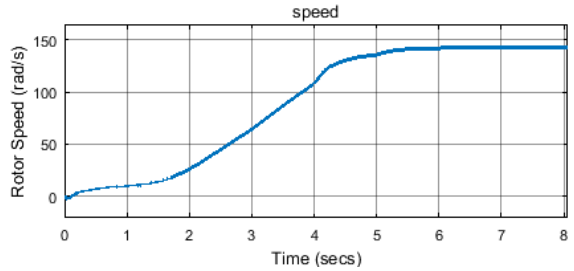

Fig.8: Rotor Mechanical Speed

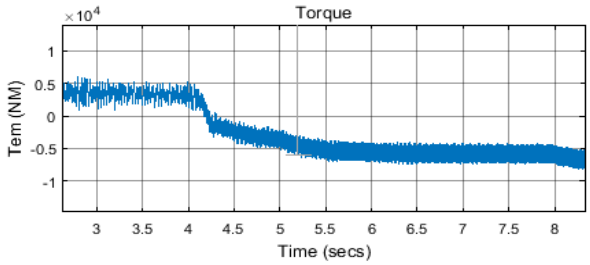

Fig. 9: Electromagnetic Torque

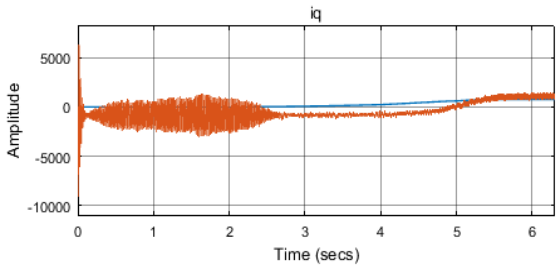

(a).

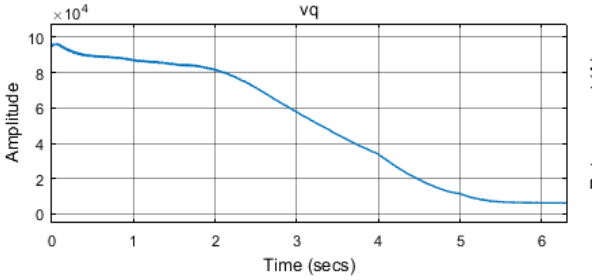

(c)

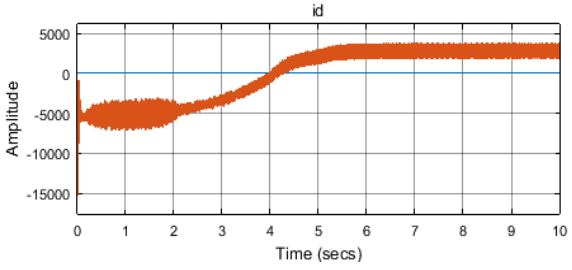

(b)

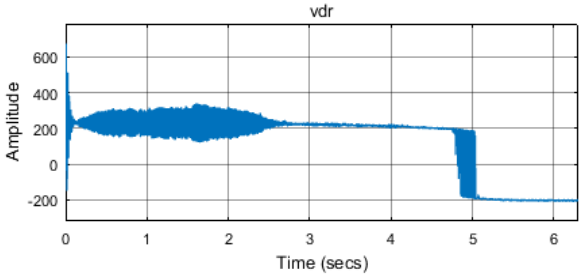

(d)

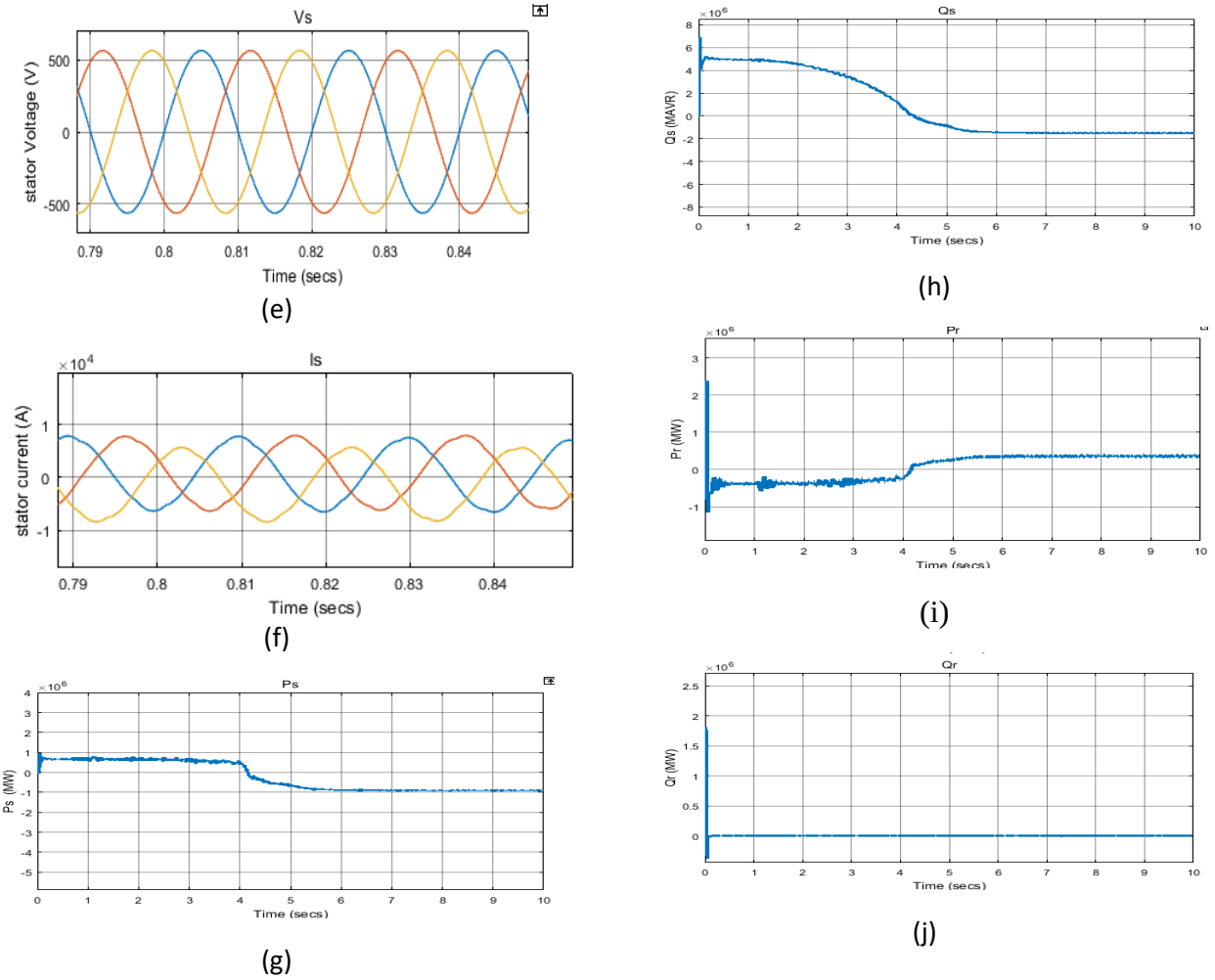

Fig. 10: The simulation results for the system at 8m/s of wind speed. (a) q- rotor current, (b) d- rotor current, (c) d- rotor voltage, (d) q- rotor voltage, (e) Stator Voltages, (f) Stator Current, (g) Active power Stator, (h) Reactive power Stator, (i) Active power Rotor (j) Reactive power Rotor..

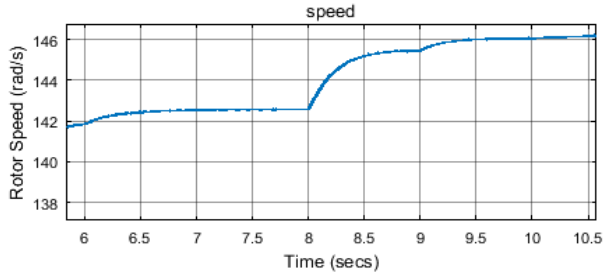

Fig. 11: (a) Step Change in Rotor speed for 8m/s to 10m/s of wind speed

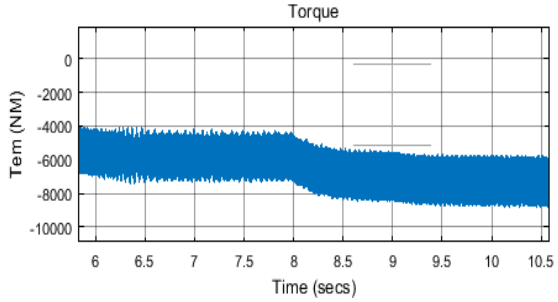

Fig. 11: (b) Step Change in Torque for 8m/s to 10m/s of wind speed

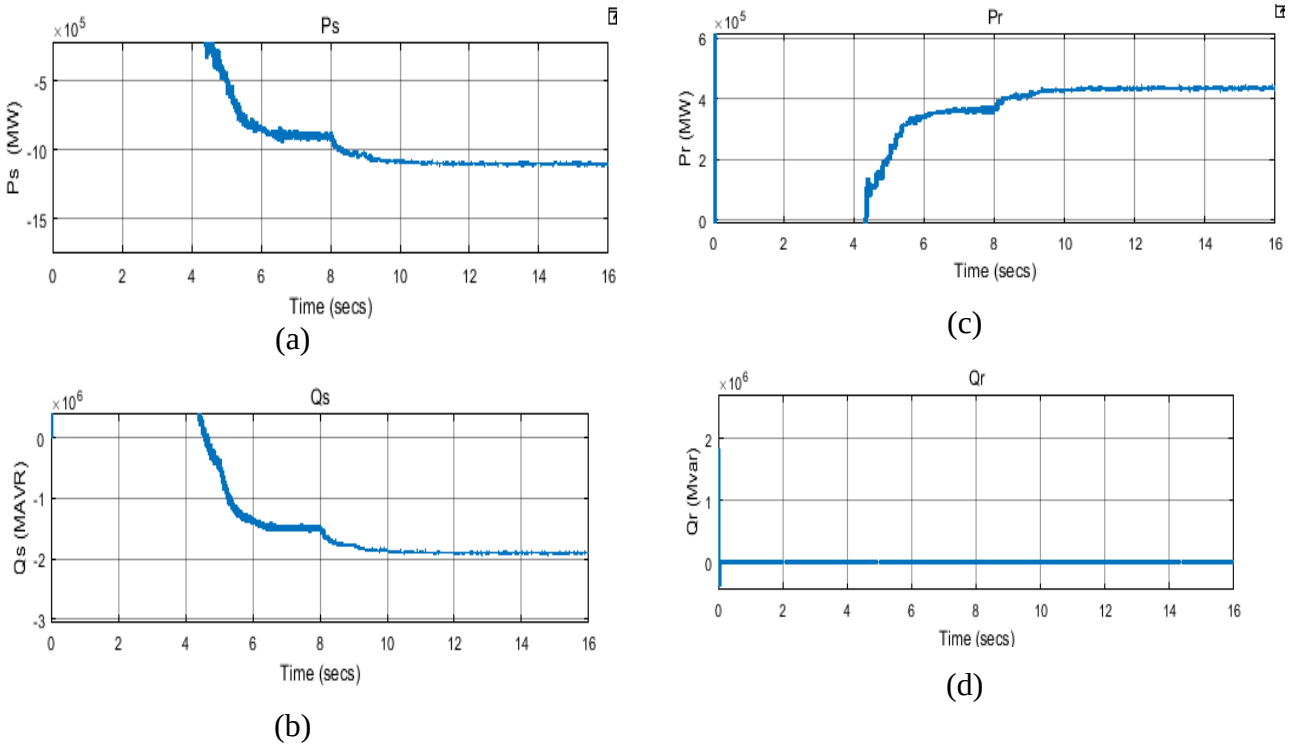

Fig. 12: The power responses with step change in te wind speed

With fluctuation of wind speed changes from 8m/s to 10m/s at simulation time t= 8 second the corresponding change in rotor mechanical speed, torque and generated power was observed in Fig. 11 and Fig. 12

MPPT control algorism is working to optimally extract power from the wind as it seen depicted in Fig. 12, when the wind speed changes to 10m/s there is an incremental change in the stator and rotor active power responses. The stator active power of Fig. 12(a) is averagely 1.1MW and from the rotor is 0.48MW as seen in Fig. 12(c) so that the grid received 1.48MW. The total active power from the practical data of the system at 10m/s of wind speed is 1.5MW as presented in Fig. 3(a) showing that the MPPT is working to track a maximum power from the wind. The reactive power response at both stator and rotor is seen in Fig. 12 (b) and (d) with reactive from the rotor at zero due to control of reactive power at the grid side inverter. The performance of the converter at the grid side was achieved by means of which the voltage at the DC bus is maintained at 1150v as shown Fig.13 (a) and the grid current from GSC was presented in Fig. 13(b).

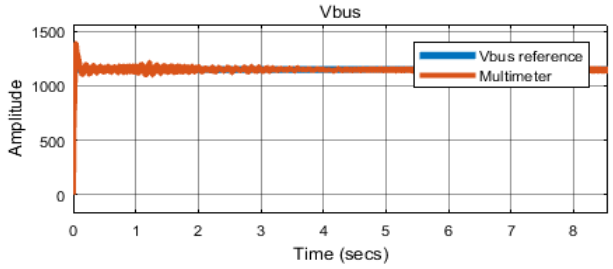

(a) The DC- bus Voltage

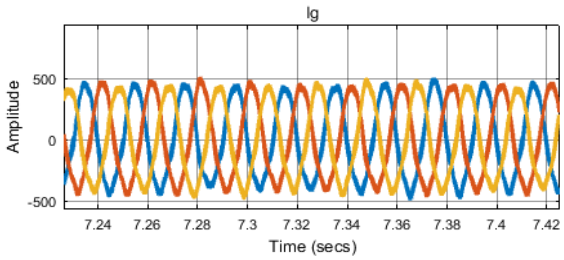

(b) GSC grid side current

Fig. 13: DC-bus Voltage and Grid Current of GSC

4. CONCLUSION

The paper evaluates the performance of a DFIG-based wind turbine in MATLAB/Simulink under two different wind speeds. The system model was made up of the aerodynamically three blades wind turbine, DFIG and bidirectional converter that drive the rotor circuit. The DFIG was modeled in a $d-q$ synchronous reference frame under stator flux orientation for which d-axis is aligned. MPPT control algorithm was applied to the wind turbine for which the system has extract the maximum energy from the wind. From the simulated results, it is evident that the system can operate under different wind conditions effectively.

REFERENCES

[1] Babu, B.C. and K. Mohanty, *Doubly-fed induction generator for variable speed wind energy conversion systems-modeling & simulation.* International Journal of Computer Electrical Engineering, 2010. **2**(1): p. 141.

[2] Liu, X. and X. Kong, *Nonlinear Model Predictive Control for DFIG-based Wind Power Generation.* IEEE Transactions on Automation Science Engineering, 2014. **11**(4): p. 1046-1055.

[3] GWEC, G.W.E.C., *Global wind report: Annual market update 2015*. URL http://gwec.net/global-figures/graphs/, 2014.

[4] Bayat, M.M. and Y. Torun. *Modeling and linearization of DFIG based wind turbine*. in *6th EURASIAN MULTIDISCIPLINARY FORUM, EMF 2017 27-28 April, Vienna, Austria*. 2017.

[5] Sediki, H., et al., *Steady-state analysis and control of double feed induction motor*. World Academy of Science, Engineering Technology, 2012. **6**(1): p. 153-161.

[6] Yang, S.-Y., et al., *Integrated Mechanical and Electrical DFIG Wind Turbine Model Development.* IEEE Transactions on Industry Applications, 2014. **50**(3): p. 2090-2102.

[7] Chatterjee, D. and Z.H. Rather, *Modelling and Control of DFIG-based Variable Speed Wind Turbine.* Indian Academy of Sciences, Bengaluru, India, 2018.

[8] Lavanya, N., O.C. Sekhar, and M. Ramamoorty. *Performance of Indirect Matrix Converter with Improved Control Feeding to Induction Mmotor for Speed Control by using PI and Fuzzy Controllers*. in *TENCON 2017-2017 IEEE Region 10 Conference*. 2017. IEEE.

[9] Amor, W.O. and M. Ghariani. *Modelling and Simulation for Variable Speed Wind Energy Conversion Systems based on Doubly-Fed Induction Generator*. in *2014 International Conference on Electrical Sciences and Technologies in Maghreb (CISTEM)*. 2014. Tunis, Tunisia: IEEE.

[10] Acakpovi, A. and E.B. Hagan, *A wind turbine system model using a doubly-fed induction generator (DFIG).* International Journal of Computer Applications, 2014. **90**(15).

[11] Abbas, F.A.R. and M.A. Abdulsada, *Simulation of wind-turbine speed control by MATLAB.* International Journal of Computer Electrical Engineering, 2010. **2**(5): p. 1793-8163.

[12] Khan, I., et al., *Dynamic Modeling and Robust Controllers Design for Doubly Fed Induction Generator-Based Wind Turbines Under*

Unbalanced Grid Fault Conditions. Energies, 2019. **12**(3): p. 454.

[13] Sleiman, M., et al. *Modeling, Control and Simulation of DFIG for Maximum Power Point Tracking*. in *2013 9th Asian Control Conference (ASCC)*. 2013. Istanbul, Turkey: IEEE.

[14] Meera, G. and N. Divya, *Rotor Side Converter Control of DFIG based Wind Energy Conversion System.* International Journal of Engineering Research & Technology (IJERT), 2015. **4**(8).

[15] Alaboudy, A.H.K., A.M. Azmy, and W.S. Abdellatif. *Controller performance of variable speed wind driven doubly-fed induction generator*. in *2015 Saudi Arabia Smart Grid (SASG)*. 2015. IEEE.

[16] Edrah, M., K.L. Lo, and O. Anaya-Lara, *Reactive Power Control of DFIG Wind Turbines for Power Oscillation Damping under a wide range of operating Conditions.* IET Generation, Transmission Distribution, 2016. **10**(15): p. 3777-3785.

[17] Abad, G., *Power electronics and electric drives for traction applications*. 2017: Wiley Online Library.

[18] Badreldien, M.M., et al. *Modeling, Analysis and Control of Doubly Fed Induction Generators for Wind Turbines*. in *The International Conference on Electrical Engineering*. 2014. Military Technical College